AJNR

Small-Vessel Stents for Intracranial Angioplasty: In Vitro Comparison of Different Stent Designs and Sizes by Using CT Angiography

Stefan Hähnel, Manuel Trossbach, Cora Braun, Sabine Heiland, Michael Knauth, Klaus Sartor and Marius Hartmann

AJNR Am J Neuroradiol 2003, 24 (8) 1512-1516
http://www.ajnr.org/content/24/8/1512

AJNR Am J Neuroradiol 24:1512–1516, September 2003

Small-Vessel Stents for Intracranial Angioplasty: In Vitro Comparison of Different Stent Designs and Sizes by Using CT Angiography

Stefan Hähnel, Manuel Trossbach, Cora Braun, Sabine Heiland, Michael Knauth, Klaus Sartor, and Marius Hartmann

BACKGROUND AND PURPOSE: **Our purpose was to evaluate whether CT angiography is a suitable alternative to conventional angiography in the evaluation of small-vessel stents for intracranial angioplasty.**

METHODS: **CT angiographic appearances of 23 stents of different designs and sizes (2.0, 3.0, and 4.0 mm) were investigated after they were filled with a solution of 0.9% NaCl or diluted contrast medium. For each stent, artificial lumen narrowing (ALN) was measured, and the difference in the number of pixels with a Hounsfield value below 200 HU between the two filling states, $DIFF_{HU<200}$, was calculated to provide an objective indicator of the size of the evaluable stent diameter.**

RESULTS: **With a window width of 1500 HU at a window level of 400 HU, ALN ranged from 66.8% to 97.7% in the group of 2.0-mm stents and from 38.6% to 66.8% in the groups of 3.0- and 4.0-mm stents. For the 2.0-mm stents, $DIFF_{HU<200}$ was zero. In the groups of 3.0- and 4.0-mm stents, $DIFF_{HU<200}$ ranged from 0.3 to 6.7, corresponding to a diameter of 0.13–3.0 mm, when the pixel size was presupposed to be 0.449 mm.**

CONCLUSION: **CT angiographic evaluation of small-vessel patency after stent placement is considerably impaired by ALN. Stent manufacturers should be aware of potential artifacts caused by their stents during noninvasive diagnostic studies such as CT angiography.**

One major problem of angioplasty with stent placement is the occurrence of in-stent neointimal growth, which can result in hemodynamically relevant restenosis or occlusion of the stented vessel segment (in-stent restenosis). The method of choice for the detection of restenosis within stented cerebral vessel segments is intra-arterial conventional angiography. This method is associated with an incidence of neurologic complications of about 0.5% (1, 2) and an incidence of clinically silent brain lesions of about 20% (3). To our knowledge, no systematic report has been published to describe artificial lumen narrowing (ALN) in small-vessel stents, as measured with CT angiography. The aim of our study was to determine whether CT angiography is suitable as a noninvasive alternative to conventional angiography in the evaluation of small-vessel stents used for intracranial angioplasty. Of particular interest was the measurement of ALN caused by the stent material within the stented vessel segment to determine whether CT angiography can be used to detect restenosis within the stent.

Received March 4, 2003; accepted after revision April 30.

From the Division of Neuroradiology, Department of Neurology, University of Heidelberg Medical Center, Germany.

Address reprint requests to Stefan Hähnel, MD, Division of Neuroradiology, Department of Neurology, University of Heidelberg Medical Center, Im Neuenheimer Feld 400, D 69120 Heidelberg, Germany.

Methods

We examined a total of 23 stents with three different diameters (2.0, 3.0, and 4.0 mm) from six manufacturers (Table). The stents were deployed in silicone tubes (NeoLab) with an inner diameter of 2.0 mm (T2), 3.0 mm (T3), or 4.0 mm (T4). The PSI stents were deployed by means of electrolytic detachment, and all other stents were deployed by balloon inflation, as usual. Digital photographs (RDCi 500 image-capturing device; Ricoh, Tokyo, Japan) and x-ray images (Integris biplanar angiographic system; Philips, Best, the Netherlands; tube voltage, 80 kV; tube current,1.5 mAs; diameter of the x-ray image amplifier, 17 cm; focus-film distance, 90 cm) were taken of the stented tubes (Fig 1). Afterward, the stented tubes were placed in a phantom parallel to the *z* axis of the CT scanner (Somatom Volume Zoom; Siemens, Forchheim, Germany). The phantom contained a solution of 0.9% NaCl. Each stented tube was axially scanned after the tube was filled with a solution of 0.9% NaCl and also after the tube was filled with diluted contrast medium (Imeron; Bracco-Byk Gulden, Konstanz, Germany) (Fig 1). For this imaging, one volume part of contrast medium was mixed with 50 volume parts of a solution of 0.9% NaCl, resulting in a fluid with a mean attenuation of 200 HU. All CT measurements were performed according to the same protocol

Properties of the analyzed stents

Stent or Tube	Trade Name	Manufacturer	Material	Stent Design	Nominal Stent Length, mm	Diameter, mm		Strut Thickness, mm	Strut Width, mm	Stent Free Area, %
						Nominal	D_{xray}*			
2.0 mm										
AVE2	AVE S660	Medtronic, Minneapolis, MN	SS 316 L	Modular	9	2.5	2.17	0.128	0.153	80
BSV2a	BioDivYsio SV	Abbott Vascular Devices, Mervue, UK	SS 316 L	Modular	10	2.0	1.96	0.091	0.08	85–90
BSV2b	BioDivYsio SV	Abbott Vascular Devices, Mervue, UK	SS 316 L	Modular	10	2.5	2.34	0.091	0.08	85–90
NLI2	Neurolink	Guidant, Indianapolis, IN	SS 316 L	MC	8	2.0	2.14	0.094	0.127	85
PSI2	PSI-Stent	Dendron, Bochum, Germany	Nitinol	SHCA	20	2.0	1.91	0.06	0.06	85
TSU2	Tsunami	Terumo, Tokyo, Japan	SS 316 L	MC	15	2.0	2.17	0.08	0.09	75
VFL2	V-Flex Plus	Cook, Bloomington, IN	SS 316 L	MC	16	2.5	1.97	0.08	0.08	>85
3.0 mm										
AVE3	AVE S670	Medtronic, Minneapolis, MN	SS 316 L	Modular	9	3.0	2.98	0.128	0.154	77–83
BAS3	BioDivYsio AS	Abbott Vascular Devices, Mervue, UK	SS 316 L	MC-modular	15	3.0	3.04	0.091	0.08	NA
BOC3	BioDivYsio OC	Abbott Vascular Devices, Mervue, UK	SS 316 L	MC-modular	28	3.0	3.24	0.091	0.08	88–91
NLI3	Neurolink	Guidant, Indianapolis, IN	SS 316 L	MC	8	3.0	3.26	0.094	0.127	87
PSI3	PSI-Stent	Dendron, Bochum, Germany	Nitinol	SHCA	20	3.0	2.83	0.06	0.06	85
TSU3	Tsunami	Terumo, Tokyo, Japan	SS 316 L	MC	15	3.0	3.04	0.08	0.09	83
VFL3	V-Flex Plus	Cook Bloomington, IN	SS 316 L	MC	12	3.0	3.04	0.08	0.08	>85
4.0 mm										
AVE4	AVE S670	Medtronic, Minneapolis, MN	SS 316 L	MC-modular	12	4.0	3.91	0.128	0.154	77–83
BAS4a	BioDivYsio AS	Abbott Vascular Devices, Mervue, UK	SS 316 L	MC-modular	15	4.0	4.13	0.091	0.08	75–81
BAS4b	BioDivYsio AS	Abbott Vascular Devices, Mervue, UK	SS 316 L	MC-modular	11	4.0	3.91	0.091	0.08	75–81
BOC4a	BioDivYsio OC	Abbott Vascular Devices, Mervue, UK	SS 316 L	MC-modular	28	3.5	4.10	0.091	0.08	88–91
BOC4b	BioDivYsio OC	Abbott Vascular Devices, Mervue, UK	SS 316 L	MC-modular	28	4.0	4.07	0.091	0.08	88–91
NLI4	Neurolink	Guidant, Indianapolis, IN	SS 316 L	MC	8	4.0	4.13	0.094	0.127	88
PSI4	PSI-Stent	Dendron, Bochum, Germany	Nitinol	SHCA	20	4.0	3.62	0.06	0.06	85
TSU4	Tsunami	Terumo, Tokyo, Japan	SS 316 L	MC	15	4.0	3.91	0.08	0.09	88
VFL4	V-Flex Plus	Cook, Bloomington, IN	SS 316 L	MC	12	3.5	4.13	0.08	0.08	>85
Tube										
T2	Tube 2 mm	NeoLab, Heidelberg, Germany	Silicone	NA	NA	2.0	NA	NA	NA	NA
T3	Tube 3 mm	NeoLab, Heidelberg, Germany	Silicone	NA	NA	3.0	NA	NA	NA	NA
T4	Tube 4 mm	NeoLab, Heidelberg, Germany	Silicone	NA	NA	4.0	NA	NA	NA	NA

Note.—MC indicates multicellular; NA, not applicable; SHCA, semihelical coil array; and SS, stainless steel.

* The diameter of each stent after balloon inflation was calculated on the basis of a radiopaque reference scale that was simultaneously x-ray imaged with the stented tube.

(detector collimation, 2 × 0.5 mm; table feed per rotation, 1.2 mm; imaging matrix, 512 × 512; section thickness, 0.5 mm; field of view, 230 mm; tube voltage, 120 kV; tube current, 300 mA; rotation time, 500 msec; convolution kernel H40fS9C0). The in-plane pixel size was 0.449 × 0.449 mm. The diameter of each stent after balloon inflation was calculated on the basis of a radiopaque reference scale that was simultaneously x-ray imaged with the stented tube. This diameter (D_{xray}) was calculated by using the medical imaging software OSIRIS (available at *www.expasy.org/UIN/html1/projects/osiris/DownloadOsiris.html*).

Subjective Evaluation

The apparent stent diameter was measured in three consecutive sections along the *x* and *y* axes, that is, perpendicular to the tube wall when the tubes were filled with diluted contrast medium. From these six measurements, the mean value and the SD were calculated. The mean stent diameter, as measured at a window width of 500 HU and a window level of 200 HU (the recommended standard window for CT angiography), was defined as $D_{500/200}$. The mean stent diameter at a window width of 1500 HU and a window level of 400 HU was defined as $D_{1500/400}$. From these data, ALN was calculated for each stent and window setting as follows: $ALN_{500/200} = [1 - (D_{500/200}/D_{xray})] \times 100\%$, and $ALN_{1500/400} = [1 - (D_{1500/400}/D_{xray})] \times 100\%$. ALN was also calculated for each tube without a stent as follows: $ALN_{500/200} = [1 - (D_{500/200}/D_{tube})] \times 100\%$, and $ALN_{1500/400} = [1 - (D_{1500/400}/D_{tube})] \times 100\%$, where D_{tube} is the accompanying inner diameter of the silicone tube.

Objective Evaluation

The attenuation of each stented tube segment was semiautomatically measured in three consecutive sections along the *x* and *y* axes on a pixel-by-pixel basis and by using the medical imaging software OSIRIS when the tubes were filled with only NaCl solution or with diluted contrast medium. From these 12 measurements, we calculated the mean difference of the number of pixels with Hounsfield values below 200 between these two filling states, as follows: $DIFF_{HU<200} = \Sigma PN_{HU<200(NaCl)}/6 - \Sigma PN_{HU<200(CM)}/6$, where $\Sigma PN_{HU<200(NaCl)}$ is the sum of the pixels with Hounsfield values below 200 HU along the *x* and *y* axes in the three consecutive sections when the tube was filled with only NaCl solution. $\Sigma PN_{HU<200(CM)}$ is the sum of the pixels with Hounsfield values below 200 HU along the *x* and *y* axes in the three consecutive sections when the tube was filled with diluted contrast medium (Fig 2). $DIFF_{HU<200}$ indicated the size of the evaluable stent diameter. Those parts of the stent lumen that could not be evaluated because of exaggerated thickening or blooming of the stent struts were not expected to have a change in their Hounsfield value between the two filling states.

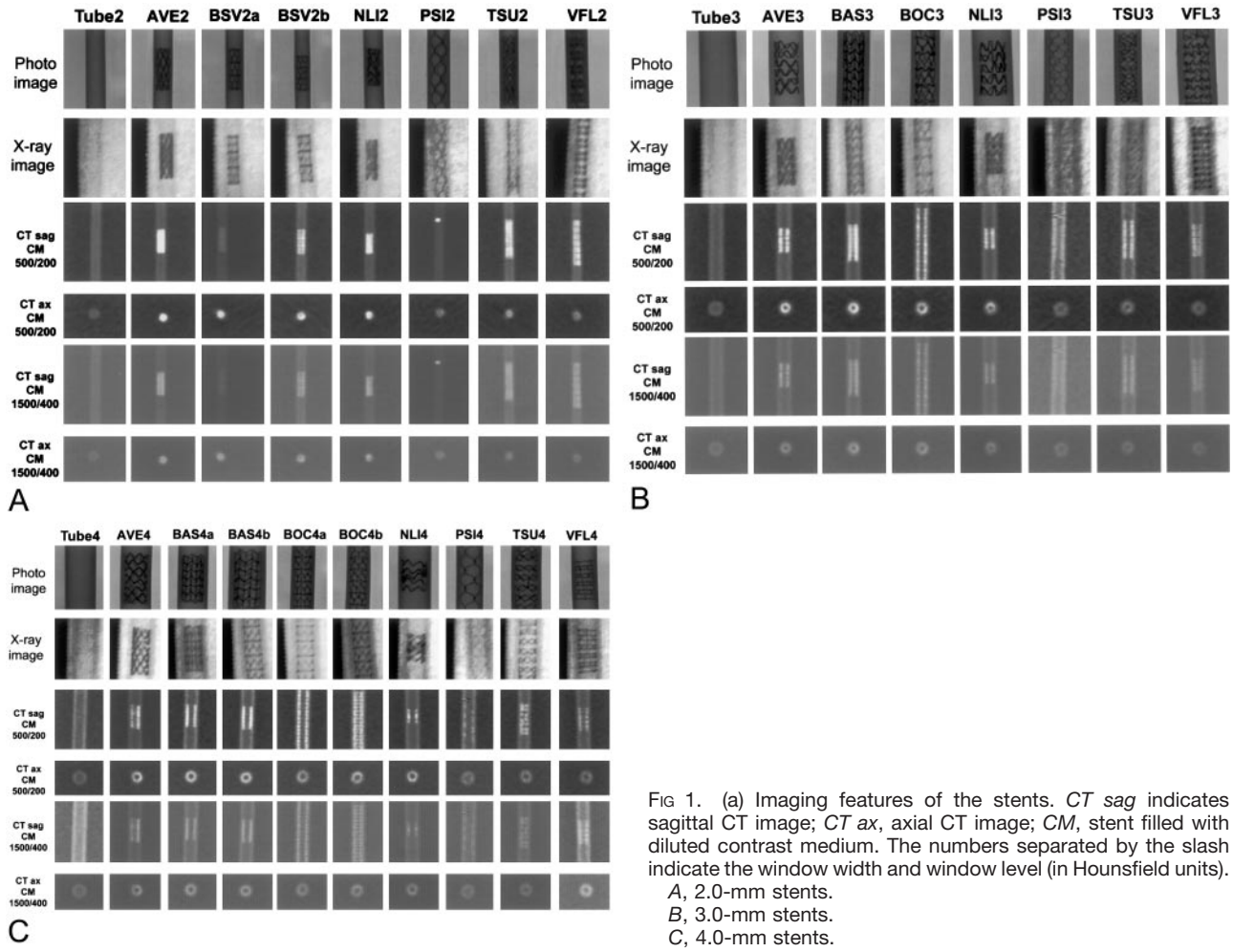

FIG 1. (a) Imaging features of the stents. *CT sag* indicates sagittal CT image; *CT ax*, axial CT image; *CM*, stent filled with diluted contrast medium. The numbers separated by the slash indicate the window width and window level (in Hounsfield units).
A, 2.0-mm stents.
B, 3.0-mm stents.
C, 4.0-mm stents.

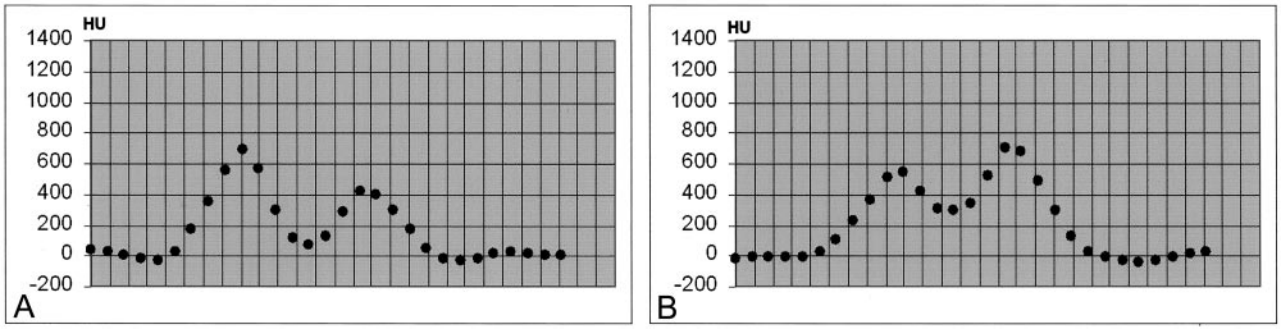

FIG 2. Attenuation profile of the BOC3 stent. The difference between two *vertical lines* represents a distance of 0.5 mm.
A, BOC3 filled with only NaCl solution only. $PN_{HU<200(NaCl)} = 3$.
B, BOC3 filled with diluted contrast medium. $PN_{HU<200(CM)} = 0$.

Results

Subjective Evaluation

In all stents, an exaggerated thickening or blooming of the stent struts was observed on the CT images, resulting in ALN of the stented tubes. In contrast to all other stents, which had an approximately symmetric design along the *z* axis, the PSI stents caused a clearly visible asymmetric CT artifact at the proximal end of the stent induced by the detachment zone (Fig 1). $ALN_{500/200}$ and $ALN_{1500/400}$ are shown in Figure 3. Generally, ALN was higher with a window width of 500 HU at a window level of 200 HU, the recommended standard window for CT angiography, as compared with a window width of 1500 HU at window level of 400 HU. There was no lumen visibility of the 2.0-mm stents with a window width of 500 HU at a window level of 200 HU. In the group of stents that were placed into the 2.0-mm tubes (2.0-mm stents), $ALN_{1500/400}$ ranged from 66.8% (BSV2a) to 97.7% (AVE2). In the group of the stents that were placed into the 3.0-mm tubes (3.0-mm stents), $ALN_{1500/400}$

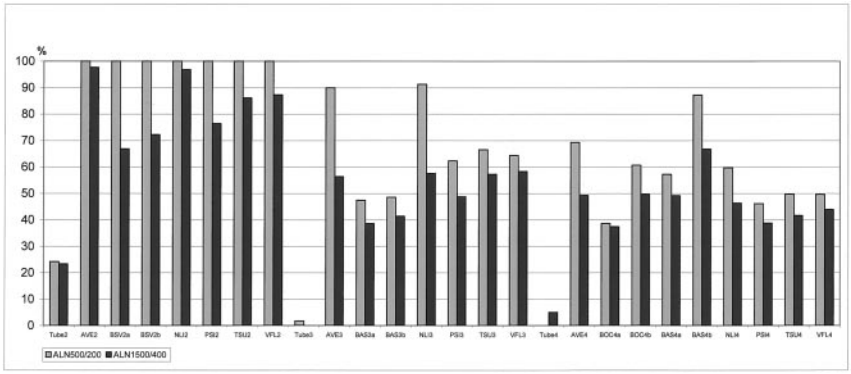

FIG 3. ALN of the stents and tubes when filled with diluted contrast medium. $ALN_{1500/400}$ was 0% for T3, and $ALN_{500/200}$ was 0% for T4.

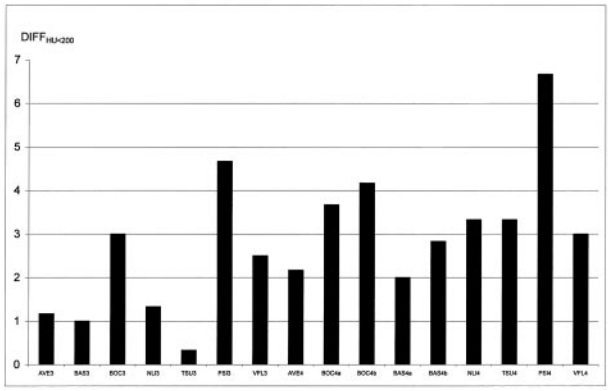

FIG 4. $DIFF_{HU<200}$ of the stents. $DIFF_{HU<200}$ was zero for all 2.0-mm stents.

ranged from 38.6% (BAS3) to 58.3% (VFL3). In the group of the stents that were placed into the 4.0-mm tubes (4.0-mm stents), $ALN_{1500/400}$ ranged from 37.4% (BOC4a) to 66.8% (BAS4b) (Fig 3). Regarding the silicone tubes, $ALN_{1500/400}$ was 23.3% for T2, 0% for T3, and 5.0% for T4. The standard deviation ranged from 0 to 0.50 for all measurements.

Objective Evaluation

The Hounsfield values within the lumen of the stented tubes increased to above zero to a variable degree, even when the stented tubes were filled with only NaCl solution (Fig 2A). Furthermore, the attenuation within the lumen of the stented tubes increased above 200 HU to a variable degree when the tubes were filled with diluted contrast medium (Fig 2B). In the group of 2.0-mm stents, $DIFF_{HU<200}$ was zero for all stents. In the group of 3.0-mm stents, $DIFF_{HU<200}$ ranged from 0.3 (TSU3) to 4.7 (PSI3), and in the group of 4.0-mm stents, $DIFF_{HU<200}$ ranged from 2.0 (BAS4a) to 6.7 (PSI4) (Fig 4).

Discussion

To determine whether CT angiography can be used as a noninvasive alternative to conventional angiography for the detection of restenosis within the stent, we evaluated the CT features of various small-vessel stents that are suitable for intracranial application. Because vessel contrast in CT angiography is exclusively based on the difference between the attenuation of the vessel filled with contrast medium and the attenuation of the surrounding tissue, and not on blood flow phenomena, our static phantom design is well suited to simulate CT angiography. In all stents, CT revealed an exaggerated thickening or blooming of the stent struts, resulting in ALN of the stented tubes. In accordance with other groups (4), we found that the Hounsfield values within the lumen of the stented tubes had increased to above zero to a variable degree even when the stented tubes were filled with only NaCl solution (Fig 2A). Furthermore, the attenuation within the lumen of the stented tubes had increased to above 200 HU to a variable degree when the tubes were filled with diluted contrast medium (Fig 2B). This increase in attenuation in the stented tubes and ALN can both be explained as compensation effects of the beam-hardening artifacts implemented in the CT reconstruction algorithm (4, 5). The strongest ALN was observed in the group of 2.0-mm stents (66.8–97.7%). ALN in the group of the 3.0-mm stents (38.6–58.3%) and in the group of the 4.0-mm stents (37.4–66.8%) was in the same range. Generally, ALN was stronger with a window width of 500 HU at a window level of 200 HU, which is the recommended standard window for CT angiography, as compared with a window width of 1500 HU at window level of 400 HU. As other groups (4), we also prefer the latter window setting for the evaluation of stents with CT angiography. In our division, patients with in-stent restenoses are treated with balloon angioplasty if they present with clinical symptoms while receiving drug therapy and if the stenoses are 50% or more according to the North American Symptomatic Carotid Endarterectomy Trial criteria (6). With the exception of the ALN for 2.0-mm stents, the ALN of the stents with which we have experience (AVE3, AVE4, NLI3, NLI4, TSU3, TSU4) was in the range of 41.6% (TSU4) to 57.6% (NLI3) (Fig 3). For the 2.0-mm stents that we used (AVE2, NLI2, TSU2), ALN was in the range of 86.2% (TSU2) to 97.9% (AVE2) (Fig 3). Therefore, an in-stent vessel stenosis would have to exceed at least 42% to be seen, and such a stenosis can be detected with CT angiography only in stented vessels with diameters of at least 3.0 mm. However, the detectability of an in-stent restenosis also depends on other factors, such as the attenuation of the con-

trast medium, spatial resolution of the CT scanner, morphology of the stenosis (eccentric or concentric), cause of the stenosis (neointimal growth or vessel thrombosis), and others. The simulated blood attenuation of 200 HU, as applied in our study, was the result of measurements obtained during in vivo CT angiography. Strotzer et al (4) have measured ALNs of 4.4–77.8% in a variety of stents with nominal diameters in the range of 8–10 mm. In our study, the attenuation within the stented tube lumen was semiautomatically measured along the *x* and *y* axes after the tubes were filled with a solution of only 0.9% NaCl and after the tubes were filled with diluted contrast medium. From these data, we calculated $DIFF_{HU<200}$ to provide an objective criterion for the size of the evaluable stent diameter. Those parts of the stent lumen that cannot be evaluated because of exaggerated thickening or blooming of the stent struts are not expected to have a change in their Hounsfield values between these two filling states. In the group of the 2.0-mm stents, pixels with values below 200 HU were not present, even if the tubes were filled with a solution of only 0.9% NaCl. In the other groups, the evaluable stent diameter was largest in the PSI stents (Fig 4). $DIFF_{HU<200}$ was 4.7 for the PSI3 stent and 6.7 for the PSI4 stent, corresponding to diameters of 2.1 and 3.0 mm, respectively, when the pixel size is assumed to be 0.449 mm, as in our study. The most likely reason for the fact that $DIFF_{HU<200}$ was clearly higher in the PSI stent than in the other stents is that the PSI stents are designed as a semihelical coil and do not have a modular or multicellular design like the other stents (Table, Fig 1). For the stents we used in intracranial angioplasty (AVE3, AVE4, NLI3, NLI4, TSU3, TSU4), $DIFF_{HU<200}$ was in the range of 0.3 (TSU3) to 3.3 (NLI4, TSU4) (Fig 4), corresponding to diameters of 0.13 and 1.48 mm, respectively. Obvious differences were noted between the subjective and objective evaluations of the stents regarding their ranking (Figs 3, 4). In our opinion, there is one important explanation for this: The subjective evaluation was based on the measurement of the stent diameters, not only on the CT images but also on the x-ray images. Therefore, if the stent struts are difficult to identify on the x-ray image, as was the case for the struts of the PSI3 stent relative to the TSU3 or BAS3 stents, for instance (Fig 1B), this effect could lead to an underestimation of D_{xray} (Table) and, thus, to an underestimation of ALN. With the exception of the PSI stents, all stents examined are made of stainless steel 316 L (Table). In contrast to all of other stents we examined in this study, the PSI stents are not primarily developed for intracranial angioplasty, but rather, for stent-covered coil embolization of cerebral aneurysms. The PSI stents are electrolytically detachable stents not yet approved for clinical application. The material of the PSI stents is nitinol, a nickel-titanium alloy (7).

Our study was performed in vitro; therefore, it has several limitations. First, the stents were scanned only axially. In oblique scanning orientations and in vessels with curved or irregular walls, ALN might be even more pronounced than it was in our study. Second, the proximal intracranial arteries have considerable movement in patients, even when the patient is completely still, and the arteries into which these devices are placed often contain calcification in their walls. Third, despite being an objective criterion for the comparison of the different stents, $DIFF_{HU<200}$ is an arbitrary parameter that does not exactly reflect the dimensions of the evaluable diameter of the stents. Fourth, as other groups (4) did, we used silicone tubes to simulate the vessel wall. The mean attenuation of the silicone walls of the tubes used in our study was 280 HU. Therefore, the tubes themselves induced ALN to a moderate degree (Fig 3). All of these limitations preclude the direct transfer of our findings to imaging results in humans.

Conclusion

Our study results show that it is necessary to know about ALN in stented vessels. Our data might influence the selection criteria for CT angiography in patients who are treated with stents not only in the cranial vessels but also in the coronary arteries. Stent manufacturers should be aware of the potential artifacts caused by these devices during noninvasive diagnostic examinations, such as CT angiography.

References

1. Grzyska U, Freitag J, Zeumer H. **Selective cerebral intraarterial DSA: complication rate and control of risk factors.** *Neuroradiology* 1990;32:296–299
2. Waugh JR, Sacharias N. **Arteriographic complications in the DSA era.** *Radiology* 1992;182:243–246
3. Bendszus M, Koltzenburg M, Burger R, Warmuth-Metz M, Hofmann E, Solymosi L. **Silent embolism in diagnostic cerebral angiography and neurointerventional procedures: a prospective study.** *Lancet* 1999;354:1594–1597
4. Strotzer M, Lenhart M, Butz B, Volk M, Manke C, Feuerbach S. **Appearance of vascular stents in computed tomographic angiography: in vitro examination of 14 different stent types.** *Invest Radiol* 2001;36:652–658
5. Chopra S, Ghiatas AA, Encarnacion CE, et al. **Transjugular intrahepatic portosystemic shunts: assessment with helical CT angiography.** *Radiology* 1997;202:277–280
6. Bladin CF, Alexandrova NA, Murphy J, Alexandrov AV, Maggisano R, Norris JW. **The clinical value of methods to measure carotid stenosis.** *Intl Angiol* 1996;15:295–299
7. Fischer A, Wieneke H, Brauer H, Erbel R. **Metallic biomaterials for coronary stents.** *Z Kardiol* 2001;90:251–262